PHYSICAL REVIEW B **80**, 241309(R) (2009)

Momentum-resolved tunneling into the Pfaffian and anti-Pfaffian edges

Alexander Seidel[1] and Kun Yang[2]
[1]*Department of Physics and Center for Materials Innovation, Washington University, St. Louis, Missouri 63136, USA*
[2]*NHMFL and Department of Physics, Florida State University, Tallahassee, Florida 32306, USA*
(Received 24 August 2009; revised manuscript received 1 November 2009; published 16 December 2009)

We calculate the electron spectral functions at the edges of the Moore-Read Pfaffian and anti-Pfaffian fractional quantum Hall states in the clean limit. We show that their qualitative differences can be probed using momentum resolved tunneling, thus providing a method to unambiguously distinguish which one is realized in the fractional quantum Hall state observed at filling factor $\nu=5/2$. We further argue that edge reconstruction, which may be less important in the first excited Landau level (LL) than in the lowest LL, can also be detected this way if present.

DOI: 10.1103/PhysRevB.80.241309 PACS number(s): 73.43.Jn, 71.10.Pm

I. INTRODUCTION

Fractional quantum Hall (FQH) systems represent one of the richest and most fascinating classes of interacting electron systems known to date. Possible realizations may include states supporting non-Abelian statistics, which have been proposed to allow fault-tolerant "topological" quantum computing.[1,2] However, in general the striking transport properties that gave the FQH effect its name are not sufficient to discriminate between various classes of different states that may occur at a given Landau level (LL) filling factor ν. The most hopeful experimental candidate system for a non-Abelian state is the FQH state at $\nu=5/2$.[3] Possible non-Abelian states explaining the $\nu=5/2$ plateau include the Moore-Read "Pfaffian" (Pf)[4] and its particle-hole conjugate counterpart, the "anti-Pfaffian" (AP).[5,6] These two states have very closely related bulk properties and most fundamentally differ through the physics of their edge states. Recent experiments involving quasiparticle tunneling between opposite edges across constrictions (or point contacts) have probed quasiparticle charge[7,8] and may have revealed signatures of non-Abelian statistics.[9] They do not, however, allow for a clear distinction between the Pf and AP states; in fact, only the experiment in Ref. 8 is sensitive to the difference between these two states, which shows up as a *quantitative* difference in certain power-law exponents. In this Rapid Communication we show that momentum resolved electron tunneling (MRT) through a clean and extended junction[10–13] into the edge of the $\nu=5/2$ state gives rise to *qualitative* differences in the signals and may thus be the most promising diagnostic tool to distinguish these two states from one another, as well as from other possible states.

II. EXPERIMENTAL SETUP AND PHYSICAL ASSUMPTIONS

A possible experimental setup is depicted in Fig. 1, which is currently being pursued experimentally.[14] The tunneling is between the $\nu=1/2$ edge in the second LL and the edge of a Hall droplet in a vertically separated layer, which we assume to be in a $\nu=1$ state. We will consider both copropagation and counterpropagation lead geometries, i.e., the $\nu=1$ edge state propagates along the same or opposite direction compared to that of the $\nu=5/2$ edge state. Note that the $\nu=1/2$ edge of the second LL will be contained well inside the edge of the filled lowest LL of the $\nu=5/2$ droplet (see Fig. 1). While this may complicate tunneling into this edge with other settings, in that of Fig. 1 this problem is circumvented by positioning a narrow $\nu=1$ strip on top of the $\nu=1/2$ edge. This allows tunneling into both a copropagating as well as a counterpropagating $\nu=1$ edge (see caption).

The Pfaffian edge theory consists of the sum of a massless chiral fermion and massless chiral boson Lagrangian density with copropagating velocities, $\mathcal{L}_{\mathrm{Pf}}(\psi,\phi)=\mathcal{L}_{\psi}+\mathcal{L}_{\phi}$, where

$$\mathcal{L}_{\psi}=i\psi(\partial_t+v_n\partial_x)\psi, \tag{1a}$$

$$\mathcal{L}_{\phi}=\frac{1}{2\pi}\partial_x\phi(\partial_t+v_c\partial_x)\phi, \tag{1b}$$

v_n and v_c are the neutral and the charged mode velocities, respectively. Here, $v_n \ll v_c$ is expected due to the fact that v_c is associated with the larger Coulomb energy scale, in agreement with the numerics in Refs. 15 and 16. In presenting the theory of the AP edge, we will follow Ref. 5, with the essential difference that we assume disorder to be so weak that momentum remains a good quantum number at the length and energy scales relevant to the experiment and do not include it. On the other hand, disorder has been a key ingredi-

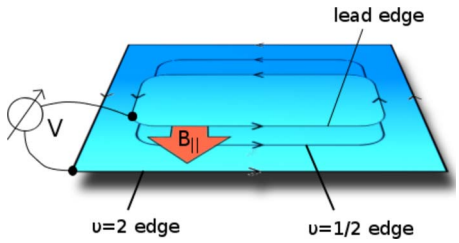

FIG. 1. (Color online) Schematic setup for momentum resolved tunneling. A $\nu=1/2$ edge in the second Landau level is contained within the outer $\nu=2$ edge of the filled lowest Landau level. Tunneling takes place between the $\nu=1/2$ edge and a lead, consisting of the edge of a narrow $\nu=1$ strip. By adjusting the position of the strip and/or the in-plane magnetic field $B_{\|}$, tunneling into a copropagating (front) or a counterpropagating (back) $\nu=1$ edge may be realized.

ent leading to the conclusion of universal scaling dimensions in Ref. 5. Here we will argue that the same universal exponents are also obtained, to very good approximation, based on the separation of energy scales between charged and neutral modes. In the spirit in Refs. 5 and 6, we thus write the theory of the AP edge as the sum of the Pfaffian edge Lagrangian with all mode velocities reversed and that of a $\nu=1$ edge, together with a density-density interaction between the two charge modes,

$$\mathcal{L}_{\mathrm{AP}} = \frac{1}{4\pi}\partial_x\phi_1(\partial_t + v_1\partial_x)\phi_1 + \bar{\mathcal{L}}_{\mathrm{Pf}}(\psi,\phi_2) + \frac{v_{12}}{2\pi}\partial_x\phi_1\partial_x\phi_2. \tag{2}$$

Here, the field ϕ_1 describes the $\nu=1$ edge and $\bar{\mathcal{L}}_{\mathrm{Pf}}$ denotes the Pfaffian Lagrangian discussed above with the formal substitution $\partial_x \to -\partial_x$. In Eq. (2), the velocity parameters and the interaction v_{12} are independent, but their relative orders of magnitude are set by the dominance of the Coulomb energy scale, as will become apparent shortly below. To see this, we carry out the charge/neutral decomposition in Ref. 5 via $\phi_\rho = \phi_1 - \phi_2$, $\phi_\sigma = \phi_1 - 2\phi_2$. The physical significance of ϕ_ρ is that $\rho_{\mathrm{tot}} = -\partial_x\phi_\rho/2\pi$ is the total charge density at the edge, while ϕ_σ is the linear combination of ϕ_1 and ϕ_2 that commutes with ρ_{tot}. In terms of the new fields,

$$\mathcal{L}_{\mathrm{AP}} = \frac{1}{2\pi}\partial_x\phi_\rho(\partial_t + v_\rho\partial_x)\phi_\rho + \frac{1}{4\pi}\partial_x\phi_\sigma(-\partial_t + v_\sigma\partial_x)\phi_\sigma + \frac{v_{\rho\sigma}}{2\pi}\partial_x\phi_\rho\partial_x\phi_\sigma + i\psi(\partial_t - v_n\partial_x)\psi, \tag{3}$$

where v_ρ, v_σ, and $v_{\rho\sigma}$ are simple linear combinations of v_1, v_c, and v_{12}. In Eq. (3), however, the large Coulomb energy scale should enter only the coupling of the total charge density with itself, i.e., v_ρ. All other coupling constants are independent of this energy scale and are expected to be much smaller, i.e., $v_\sigma \sim v_{\rho\sigma} \ll v_\rho$. Under these circumstances, the intermode coupling constant $v_{\rho\sigma}$ has a very small effect of order $v_{\rho\sigma}/v_\rho$ on the scaling dimensions of operators. To a good approximation, we may thus set $v_{\rho\sigma} \approx 0$, which allows us to read the scaling dimensions of various operators directly off Eq. (3). Here we are only interested in the most relevant operators that have the quantum numbers of the electron operator. These operators and their scaling dimension are then identical to those identified in Refs. 5 and 6. We emphasize, however, that the argument given here relies on the dominance of Coulomb interactions only and does not invoke disorder, which played a central role in Ref. 5. As a result, the edge theory [Eq. (3)] retains two distinct counterpropagating neutral mode velocities, v_n and v_σ.

III. ELECTRON OPERATORS AND SPECTRAL FUNCTIONS

An electron operator of minimal scaling dimension 3/2 is given by $\psi_{\mathrm{el},1}(x) = \psi(x)\exp[-2i\phi_\rho(x)]$ for both the AP and Pf edge theories (we identify $\phi \equiv \phi_\rho$ in the latter). In the Pf case, this is the unique leading electron operator, whereas there are two more such operators of equal scaling dimension in the AP case. These may be taken to be $\psi_{\mathrm{el},2,3}(x) = \exp[\pm i\phi_\sigma(x)]\exp[-2i\phi_\rho(x)]$. The leading term in the electron operator at the AP edge is thus a superposition of the operators $\psi_{\mathrm{el},j}$, $j=1,2,3$. However, all cross correlations between different $\psi_{\mathrm{el},j}$ vanish, and the electron Green's function is of the form $G(t,x) \simeq -i\Sigma_j a_j \langle \psi^\dagger_{\mathrm{el},j}(t,x)\psi_{\mathrm{el},j}(0,0)\rangle$. We will discuss the contributions to the electron spectral function of these correlators separately. Their real space structure is given by

$$\langle \psi^\dagger_{\mathrm{el},j}(t,x)\psi_{\mathrm{el},j}(0,0)\rangle \propto \frac{i\ \mathrm{sgn}(u_n)}{x - u_n t + i0^+\ \mathrm{sgn}(u_n t)} \frac{-1}{[x - u_c t + i0^+\ \mathrm{sgn}(t)]^2}. \tag{4}$$

In the above, u_c equals v_c in the Pf case and v_ρ in the AP case, whereas u_n equals v_n in the Pf case and $-v_n$ in the AP case for $j=1$ and $-v_\sigma$ for $j=2,3$. From Eq. (4) one can obtain the Fourier transform $G(\omega,q)$ of the electron Green's function, and the spectral function $A(\omega,q) = -(1/\pi)\mathrm{Im}\, G(\omega,q)\mathrm{sgn}(\omega)$. More directly, $A(\omega,q)$ can be obtained from the convolution method detailed in Ref. 17. For each of the leading contributions shown in Eq. (4), the result $A_j(\omega,q)$ is given by

$$A_j(\omega,q) \propto \Theta[u_n(\omega - qu_n)(qu_c - \omega)]\frac{|\omega - qu_n|}{(u_c - u_n)^2} \tag{5}$$

with Θ as the Heaviside step function.

The results are plotted in Fig. 2 for both the Pf ($u_n > 0$) and the AP ($u_n < 0$) cases. The presence or lack of a counterpropagating mode is clearly visible. This leads to different kinematic constraints on the spectral weight. In the Pfaffian copropagating case, for any given q we can make excitations only within a finite ω range between $u_n q$ and $u_c q$. In contrast, in the AP case, the presence of two mutually counterpropagating modes relevant to each A_j *excludes* the spectral weight from a finite range of frequencies at each q.

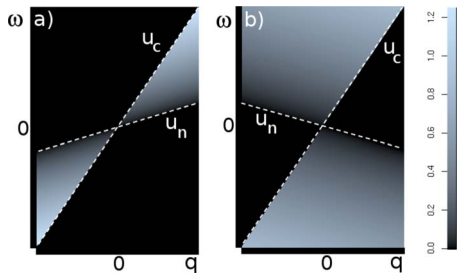

FIG. 2. (Color online) The electron spectral function in the low-energy long-wavelength limit for the (a) Pfaffian and (b) anti-Pfaffian edges. q is measured relative to the Fermi wave vector at the edge for a specific electron operator. Dashed lines indicate $\omega = u_c q$ and $\omega = u_n q$. In (b), only the contribution to the spectral function due to one of the three leading electron operators at the anti-Pfaffian edge is shown (see text).

IV. MRT CONDUCTANCE

We calculate the tunneling current in linear response using the theory discussed in Ref. 17,

$$I_j(V,\Delta q) \propto \int d\omega_1 d\omega_2 dq_1 dq_2 A_L(\omega_1,q_1) A_j(\omega_2,q_2) \times [f(\omega_1)-f(\omega_2)]\delta(eV+\omega_1-\omega_2)\delta(\Delta q+q_1-q_2). \tag{6}$$

Here $A_L(\omega,q)$ is the lead spectral function. We take $A_L(\omega,q)=\delta(\omega-u_L q)$ corresponding to a $\nu=1$ edge, with $u_L>0$ for the copropagating lead geometry and $u_L<0$ for the counterpropagating lead geometry (cf. Fig. 1), though other types of leads may be considered. $f(\omega)$ is the Fermi-distribution function, where we assume zero temperature in the following. V is the applied voltage and $\Delta q=ed(B_\parallel-B_j)/\hbar c$ is the change in the electron wave-vector relative to the Fermi wave vector, where $B_\parallel$ is the in-plane magnetic field, B_j is an offset accounting for different Fermi wave vectors in the lead and the Pf or AP edge, and d is the distance between the two layers. B_j is expected to depend on j as we will further discuss below. This may lead to additional distinctive features between the Pf and the AP cases since the total current is the superposition $I(V,B_\parallel)=\Sigma_j a_j I_j(V,\Delta q)$ in the latter. From Eq. (6), it is straightforward to evaluate $I_j(V,\Delta q)$ for various cases. We present a general result that is valid for any signs of u_n and u_L and only assumes that $|u_n|$ is smaller than the "charged" velocity parameters u_c and $|u_L|$. We consider both $u_c<u_L$ and $u_c>u_L$, which lead to qualitative differences in the copropagating lead case. The general result can be glued together from three functions, defined as

$$I_A=\frac{\mathrm{sgn}(u_L)(eV-\Delta q u_L)^2}{(u_L-u_n)(u_c-u_L)^2}, \quad I_B=\frac{\mathrm{sgn}(u_L)(eV-\Delta q u_n)^2}{(u_L-u_n)(u_c-u_n)^2},$$

$$I_C=\frac{\mathrm{sgn}(u_L)(eV-\Delta q u_c)}{(u_c-u_n)^2(u_c-u_L)^2} \times [eV(u_n+u_L-2u_c)+\Delta q(u_n u_c+u_L u_c-2u_n u_L)]. \tag{7}$$

For each of these three expressions, we define an associated interval in Δq. Let J_{AC} be the interval between eV/u_L and eV/u_c and J_B be the interval between eV/u_n and *either* eV/u_L *or* eV/u_c, whichever is closer to eV/u_n. Obviously, J_{AC} and J_B share a common boundary point and are otherwise disjoint. Equation (7) was written down with the tacit understanding that the expressions for I_A and I_C are only valid when $\Delta q \in J_{AC}$ and that for I_B is only valid for $\Delta q \in J_B$. Outside these intervals, the associated currents are defined to be zero. For $V>0$ and with these conventions, we find $I_j=I_A+I_B$ for $u_L(u_L-u_c)u_n>0$ and $I_j=I_C+I_B$ otherwise. The case $V<0$ is obtained via $I_j(V,\Delta q)=-I_j(-V,-\Delta q)$.

V. RESULTS AND DISCUSSION

Figure 3 shows our results for dI_j/dV for six cases of interest, corresponding to the Pf and AP edge states, for copropagating and counterpropagating lead geometries, and for both signs of u_L-u_c in the former case. The most striking difference between the Pf and the AP cases is apparent in the copropagating lead geometry. Here, a positive V requires a positive Δq for a current to flow in the Pf case. In contrast, a current will always flow for a range of positive and negative values of Δq in the AP case. These observations are direct consequences of the kinematic constraints on the spectral function discussed above. Furthermore, it is only in the Pf copropagating cases that dI/dV becomes negative. However, even for a counterpropagating lead, the Pf and the AP cases are clearly distinguishable. The smallest mode velocity which is visible in the graph can always be identified with u_n, and its sign distinguishes the Pf from the AP case. Also note that in Fig. 3(f) (AP, counterpropagating), dI/dV has no discontinuity *within* the region of nonzero current but does so at

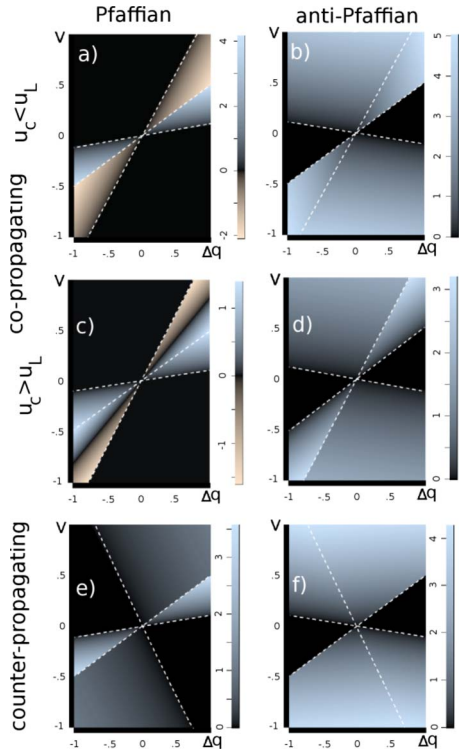

FIG. 3. (Color online) dI/dV as a function of applied voltage V and wave-number change Δq (all units are arbitrary). Δq is related to the in-plane magnetic field $B_\parallel$ via $\Delta q=ed(B_\parallel-B_j)/\hbar c$ (see text). The first column shows results for the Pfaffian case ($u_n>0$); the second column applies to the anti-Pfaffian case ($u_n<0$). The last row assumes tunneling into a counterpropagating $\nu=1$ lead edge ($u_L<0$); the first two rows assume a copropagating lead edge ($u_L>0$), with u_L greater than (less than) u_c in the first (second) row. Dashed lines correspond to $eV=u_n q$, $eV=u_c q$, and $eV=u_L q$, respectively, and mark the boundaries of different regions across which dI/dV and/or its derivatives have discontinuities. For clarity, we have chosen $|u_n|=0.1$ always, and $u_c=0.5$, $|u_L|=1.3$ for the first and last rows, whereas $u_c=1.3$ and $u_L=0.5$ in the second row. The signs of u_n and u_L are varied as appropriate to each case. Distinctive features discriminating between the Pfaffian and anti-Pfaffian cases are clearly visible. In addition, the dI/dV plots shown here for the anti-Pfaffian edge take into account only one of the three leading electron operators for simplicity. In the full dI/dV signal, each of these operators makes a contribution of the kind shown above but possibly with different horizontal offsets and with only two of the three neutral mode velocities identical (see text).

one of its boundaries. In contrast, the case in Fig. 3(e) (Pf, counterpropagating) shows a dI/dV discontinuity within the region of nonzero current but not at its boundaries. Furthermore, even in the AP counterpropagating case [Fig. 3(f)] a discontinuity in d^2I/dV^2 will clearly distinguish between two different regions (corresponding to $I_j=I_B$ and $I_j=I_C$). The separating line between these two regions has a slope, u_c, which differs in sign from the slope u_L of a similar separating line in the Pf counterpropagating case [Fig. 3(e)]. More generally, Figs. 3(b), 3(c), and 3(f) have no discontinuity in dI/dV within the region of nonzero current but have a discontinuity at one of its boundaries, in contrast to the cases in Figs. 3(a), 3(d), and 3(e). Note that in Fig. 3(b) (Pf, copropagating, $u_c > u_L$), dI/dV smoothly goes through zero within the region where $I_j=I_C$. In any case, discontinuities in either dI/dV or d^2I/dV^2 allow for a direct measurement of the edge mode velocities. These findings imply that under all circumstances considered here, the MRT conductance clearly distinguishes the Pf edge from the AP edge. This becomes even more pronounced when one takes into account that in the AP case, the MRT current is a superposition of the form $I(V,B_\parallel)=\Sigma_j a_j I_j(V,\Delta q)$. As discussed above, the contributions I_j do not all feature the same neutral mode velocity u_n in the clean case considered here. Even more importantly, the offset B_j entering the definition of Δq is expected to depend on j as well. This is so because the three operators $\psi_{\mathrm{el},j}$ will in general carry different momenta. To see this, we may reinterpret these operators in terms of processes taking place at the original $\nu=1$ edge and particle-hole conjugated Pfaffian $\nu=1/2$ edge present in Eq. (2). It is easy to see that, e.g., $\psi_{\mathrm{el},1}$ creates one electron at the $\nu=1/2$ edge while destroying two electrons at the $\nu=1$ edge. Similarly, $\psi_{\mathrm{el},2}$ simply destroys one electron at the $\nu=1$ edge. Hence, if different Fermi momenta are associated with the $\nu=1$ and $\nu=1/2$ components of the edge, all three operators $\psi_{\mathrm{el},j}$ carry different momenta. In the AP case, one thus expects to measure an MRT conductance which is the superposition of three graphs taken from the appropriate row in the second column of Fig. 3, with three different horizontal offsets and with two different neutral mode velocities u_n.

We remark that the above results could in principle be affected by edge reconstruction. However, we expect these effects to be considerably weaker at the second LL edge of interest here. Since this edge is well contained inside the physical edge of the sample, fringe field effects, which are usually associated with edge reconstruction,[16] will be weak. Hence we argue that a picture based on an unreconstructed $\nu=1/2$ edge may apply. If edge reconstruction indeed occurs, additional edge modes will result and they can in principle also be detected using the setup discussed here; see Ref. 17 for a discussion of this point in the (simpler) context of a $\nu=1/3$ edge, and a detailed study will be left for future work (see also Ref. 18). We note that we have considered the setup of Fig. 1 both for its simplicity and experimental relevance;[14] in principle other setups like those in Refs. 10–13 can also be used to study the 5/2 edge. Finally, we mention a recent alternative proposal to distinguish the Pf edge from the nonequilibrated AP edge, involving simple two-terminal measurements.[19] We caution, however, that the presence of the contacts in such experiments will almost certainly lead to disorder and equilibration among the edge channels at least near the contacts. As a result the predicted two-terminal conductance for a scenario based on nonequilibrated edges may never be observed. On the other hand, the (momentum conserving) tunneling processes we consider occur away from these contacts and thus do not suffer from the contact-induced disorder. We are thus hopeful that MRT will prove a useful tool to shed further light on the $\nu=5/2$ quantum Hall state in the future.

ACKNOWLEDGMENTS

We are indebted to M. Grayson, W. Kang, C. Nayak, and A. Yacoby for insightful discussions. This work was supported by NSF Grant No. DMR-0907793 (A.S.) and NSF Grant No. DMR-0704133 (K.Y.).

[1] A. Y. Kitaev, Ann. Phys. **303**, 2 (2003).
[2] S. Das Sarma, M. Freedman, and C. Nayak, Phys. Rev. Lett. **94**, 166802 (2005).
[3] R. Willett, J. P. Eisenstein, H. L. Störmer, D. C. Tsui, A. C. Gossard, and J. H. English, Phys. Rev. Lett. **59**, 1776 (1987).
[4] G. Moore and N. Read, Nucl. Phys. B **360**, 362 (1991).
[5] S.-S. Lee, S. Ryu, C. Nayak, and M. P. A. Fisher, Phys. Rev. Lett. **99**, 236807 (2007).
[6] M. Levin, B. I. Halperin, and B. Rosenow, Phys. Rev. Lett. **99**, 236806 (2007).
[7] M. Dolev, M. Heiblum, V. Umansky, A. Stern, and D. Mahalu, Nature (London) **452**, 829 (2008).
[8] I. P. Radu, J. B. Miller, C. M. Marcus, M. A. Kastner, L. N. Pfeiffer, and K. W. West, Science **320**, 899 (2008).
[9] R. L. Willett, L. N. Pfeiffer, and K. W. West, Proc. Natl. Acad. Sci. U.S.A. **106**, 8853 (2009).
[10] W. Kang, H. L. Stormer, L. N. Pfeiffer, K. W. Baldwin, and K. W. West, Nature (London) **403**, 59 (2000).
[11] I. Yang, W. Kang, K. W. Baldwin, L. N. Pfeiffer, and K. W. West, Phys. Rev. Lett. **92**, 056802 (2004).
[12] M. Huber, M. Grayson, D. Schuh, M. Bichler, W. Biberacher, W. Wegscheider, and G. Abstreiter, Physica E (Amsterdam) **22**, 164 (2004).
[13] M. Huber, M. Grayson, M. Rother, W. Biberacher, W. Wegscheider, and G. Abstreiter, Phys. Rev. Lett. **94**, 016805 (2005).
[14] A. Yacoby (private communication).
[15] X. Wan, K. Yang, and E. H. Rezayi, Phys. Rev. Lett. **97**, 256804 (2006).
[16] X. Wan, Z.-X. Hu, E. H. Rezayi, and K. Yang, Phys. Rev. B **77**, 165316 (2008).
[17] A. Melikidze and K. Yang, Phys. Rev. B **70**, 161312(R) (2004); Int. J. Mod. Phys. B **18**, 3521 (2004).
[18] B. Overbosch and X. Wen, arXiv:0804.2087 (unpublished).
[19] C. Wang and D. Feldman, arXiv:0909.3111 (unpublished).